Chemical Science

ROYAL SOCIETY OF CHEMISTRY

EDGE ARTICLE

View Article Online
View Journal | View Issue

Cite this: *Chem. Sci.*, 2024, **15**, 6130

All publication charges for this article have been paid for by the Royal Society of Chemistry

Received 24th January 2024
Accepted 20th March 2024

DOI: 10.1039/d4sc00581c

rsc.li/chemical-science

Intramolecular chaperone-assisted dual-anchoring activation (ICDA): a suitable preorganization for electrophilic halocyclization†

Xihui Yang, [a] Haowei Gao,[a] Jiale Yan,[a] Jia Zhou *[ab] and Lei Shi *[a]

The halocyclization reaction represents one of the most common methodologies for the synthesis of heterocyclic molecules. Many efforts have been made to balance the relationship between structure, reactivity and selectivity, including the design of new electrophilic halogenation reagents and the utilization of activating strategies. However, discovering universal reagents or activating strategies for electrophilic halocyclization remains challenging due to the case-by-case practice for different substrates or different cyclization models. Here we report an intramolecular chaperone-assisted dual-anchoring activation (ICDA) model for electrophilic halocyclization, taking advantage of the non-covalent dual-anchoring orientation as the driving force. This protocol allows a practical, catalyst-free and rapid approach to access seven types of small-sized, medium-sized, and large-sized heterocyclic units and to realize polyene-like domino halocyclizations, as exemplified by nearly 90 examples, including a risk-reducing flow protocol for gram-scale synthesis. DFT studies verify the crucial role of ICDA in affording a suitable preorganization for transition state stabilization and X^+ transfer acceleration. The utilization of the ICDA model allows a spatiotemporal adjustment to straightforwardly obtain fast, selective and high-yielding synthetic transformations.

Introduction

Halogen-induced intramolecular cyclization of unactivated alkenes has emerged as a powerful strategy to rapidly build up molecular complexity, due to the concomitant formation of a nascent heterocyclic moiety and halide functionalities.[1] However, a harmonious relationship between structure, reactivity and selectivity for electrophilic halocyclization has proven to be a long-standing problem. For example, advancements in medium-sized and large-sized halocyclization,[2] polyene-like domino halocyclization,[3] asymmetric variants of electrophilic halocyclization[4] and clear-cut reaction mechanism determination[5] remain challenging (Fig. S1 to S3†) due to the case-by-case practice for different substrates or different cyclization models. To this end, a variety of electrophilic halogenation reagents, from molecular halogens (X_2, X = Cl, Br, I) to stable and available reagents bearing the N–X bond, have been developed successively (Scheme 1a, left).[6] Nevertheless, a catalyst or an extra additive was generally required to increase the electrophilic character of *N*-haloamides, which is typically realized by Lewis/Brønsted acid activation[7] or Lewis base activation[8] (Scheme 1a, middle, and Fig. S4a†). More recently, significant efforts have also been devoted to the elaboration of practical and highly reactive electrophilic halogenation reagents, including $Et_2SX{\cdot}SbCl_5X$ (X = Br or Cl),[9] Palau'chlor[10] and Py_2IBF_4,[11] for direct halogenation (Scheme 1a, right, and Fig. S4b†). Nevertheless, the range of applications has been restricted by their incomplete halenium sources and stability liabilities from moisture, light and so on.[12] Therefore, it is desired to develop powerful electrophilic halogenation strategies that can balance the relationship between structure, reactivity and selectivity.

In the pursuit of fast, selective and high-yielding organic transformations, the proximity and orientation effects have been central chemical tenets in regulating many important biological processes.[13] The recognition site of an enzyme usually makes use of a combination of multiple non-covalent interactions to bring the substrates in spatial proximity to the reaction site and increase the reaction rate (Scheme 1b, left, and Fig. S5a†). The proximity and orientation effects allow a maximally reactive conformation of substrates and further stabilize the transition state because of the specific enzyme–substrate preorganization (Fig. S5b and S6†).[14] For an efficient and position-specific halogen installation, enzymatic halogenation reactions are generally predominated by an oxidative strategy in which an oxygen-based oxidant is utilized to oxidize halide ions

[a]*School of Science (Shenzhen), School of Chemistry and Chemical Engineering, Harbin Institute of Technology, Shenzhen 518055, China. E-mail: jiazhou@hit.edu.cn; lshi@hit.edu.cn*

[b]*Laboratory of Urban Water Resources and Environment, Harbin Institute of Technology (Shenzhen), Shenzhen 518055, China*

† Electronic supplementary information (ESI) available. See DOI: https://doi.org/10.1039/d4sc00581c

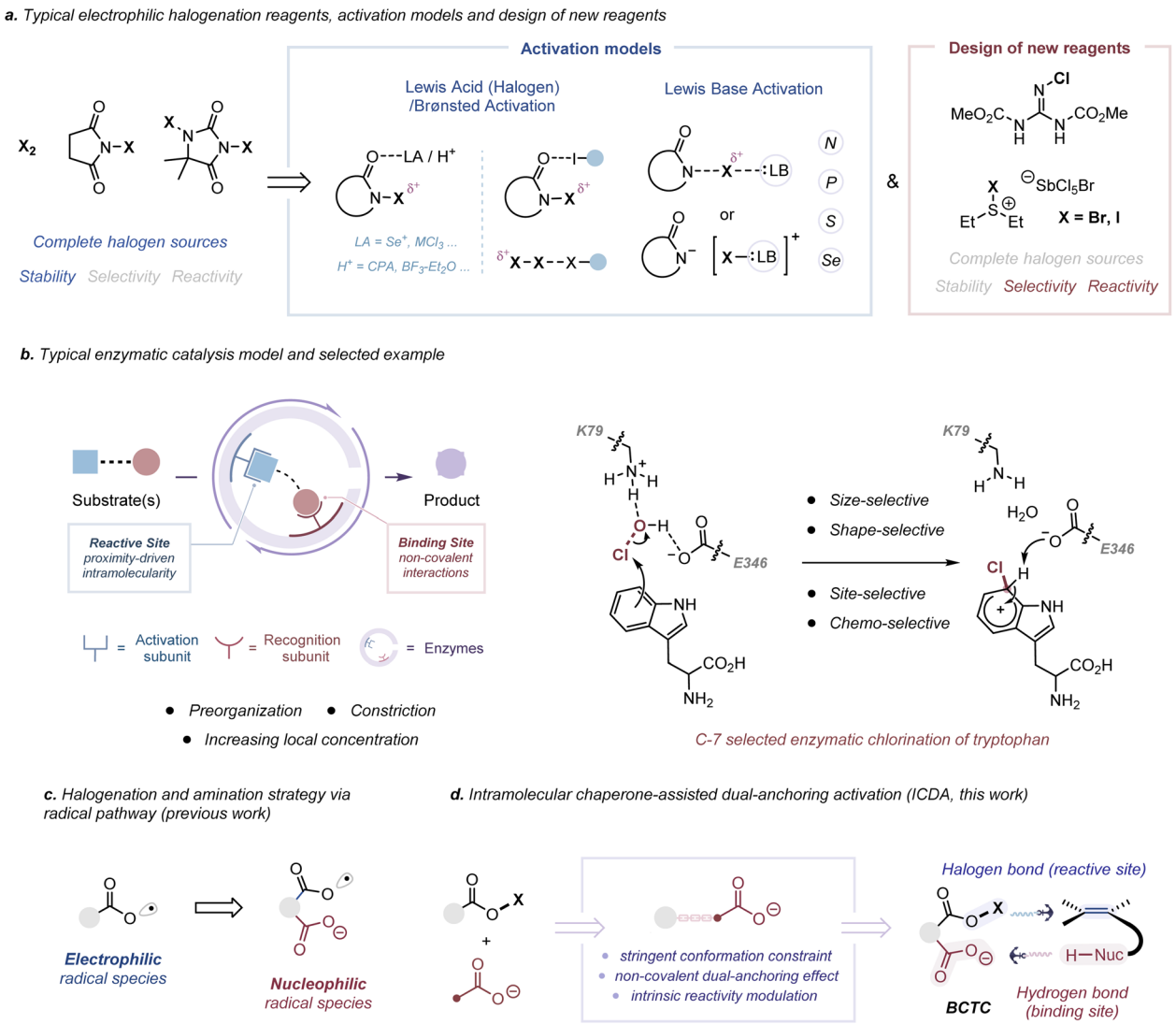

Scheme 1 Summary of halogenation reagents, enzymatic catalysis and our strategy design.

(X^-) into the corresponding hypohalite (^-OX) intermediates (Fig. S4c†).[15] In a polar pathway, these intermediates react as activated X^+ equivalents with electron-rich substrates owing to the high electrophilicity of the oxygen atom ($\chi_P = 3.44$).[16] In regard to the regioselective C-7 chlorination of tryptophan by flavin-dependent halogenases, HOCl, for example, is generated by the reaction of flavin hydroperoxide and the chloride ion (Scheme 1b, right).[17] Chlorination by free HOCl lacks both regiospecificity and substrate specificity. Before electrophilic chlorination, the K79 residue may hydrogen bond to free HOCl, thus positioning it proximal to tryptophan and increasing the electrophilicity of Cl^+. During the chlorination, the carboxylate group of the proximal E346 residue is oriented to stabilize and deprotonate the resulting Wheland intermediate, leading to a C-7 selective chlorination product. Such a spatially confined activating step may not only enable the chlorination of less reactive substrates but also protect nearby tryptophan residues.

In our previous work, we have found that the combination of phthaloyl peroxide (PPO) and X^- can generate Brønsted base Covalently Tethered Carbonyl hypohalites (BCTC) *via* an oxidative strategy.[18] Taking advantage of the spatially confined non-covalent orientation and proximity effect, our previous studies have developed a tether-tunable distonic radical anion mediated approach, wherein the installation of an intramolecular chaperone-like carboxylate anion leads to a polarity inversion or umpolung strategy, for the direct generation of heteroatom-centered radicals from O–H or N–H bonds (Scheme 1c).[18] Along these lines, except for the radical ($1e^-$) process, we envisioned that BCTC would act as an *in situ* generated electrophilic reagent in a closed shell ($2e^-$) process for halocyclization reactions. In the proposal, this protocol allows the utilization of a covalently integrated halogen bond donor and hydrogen bond acceptor for dual-anchoring orientation (Scheme 1d). At the molecular level, this Intramolecular Chaperone-assisted Dual-anchoring Activation (ICDA) model could afford an induced-fit conformational change in a tailored environment and create a specific reactive conformation, thus

pre-paying for the entropy loss required for the formation of the transition state to accelerate the reaction.[19]

Results and discussion

Optimization of the reaction conditions

To validate our hypothesis, 4-phenyl-4-pentenoic acid **1a** was selected as the model substituted alkene for optimization studies (Table 1, see more details in Tables S1 to S4†). The reaction rate of this turbo-charged bimolecular process is increased by orders of magnitude compared to the three-molecule process induced by benzoyl peroxide (BPO) (the reaction was finished in 30 s; see the video in the ESI†) *via* ICDA (Table 1, entries 1 to 4). Tetrabutylammonium bromide (TBAB) was proved to be the optimal halogen source (Table 1, entries 5 and 6, and Table S2†). Furthermore, bromolactonization of **1a** was conducted under the irradiation of a blue LED (400 nm), and the yield of **2a-Br** was decreased to 51% which might be due to the undesired radical side-reactions (Table 1, entry 7).[18b]

Synthesis of five-membered and six-membered heterocyclic rings enhanced by ICDA

With the optimized conditions in hand, we assessed the scope of alkenoic acids to test the functional group tolerance of this protocol (Scheme 2). Generally, electron-donating, electron-neutral, and electron-withdrawing substituents on 4-aryl-4-enoic acids exhibited similar tolerance: methoxy, alkyl, aryl, halo, trifluoromethyl, nitryl, cyan, methoxycarbonyl, sulfonyl, and dimethylcarbamoyl were sufficiently compatible, and the corresponding γ-lactones (**2b**–**2l**) were obtained in 80 to 96% yields within two minutes. Different steric substituted groups were found to have negligible effects on the bromolactonization (**2m**–**2p**). Pyridyl (**2q**) and alkynyl (**2r**) were compatible with the oxidizing atmosphere. The bromolactonization of α,β-unsaturated enone **1s** with a comparatively inert and sluggish π-bond was implemented successfully (**2s**, 84%).[20] Our approach is also suitable for the synthesis of 3,3-disubstituted phthalide (**2t**) and halogenated α-*exo*-methylene-lactone (**2u**). The BCTC-induced bromolactonization of substrates bearing an *endo*-cyclic π-bond (**1v**–**1z**) proceeded smoothly with exclusive diastereoselectivities superior to the previous report.[21] The bromolactonization of mono-substituted alkene **1aa** definitely furnished the *exo*-lactone **2aa** as a single diastereomer with 81% yield. The reaction of the (*Z*)-1,2-disubstituted alkene (**1ab**) proceeded with exclusive diastereoselectivity and regioselectivity. A mixture of δ-valerolactone (**2ac**) and γ-butyrolactone (**2ac′**) in a ratio of 2.3 : 1 was obtained when (*E*)-5-phenylpent-4-enoic acid (**1ac**) was used as the substrate. Furthermore, our protocol is also competent for the synthesis of six-membered lactones (**2ad**–**2ak**) and *E*-bromo enol lactone (**2al**) in 40 to 96% yields *via exo*-cyclization.

This protocol was also suitable for the synthesis of substituted tetrahydrofurans (**4a**–**4c**) in 54–89% yields. A transannular bromoetherification of **3d** allowed for the high-efficiency synthesis of 2-oxabicyclo[2.1.1]hexane, which is regarded as a saturated benzene mimetic and an analogue of bicyclo[1.1.1]pentane (BCP).[22] Additionally, multiple substituted β,γ-unsaturated allylic ketoximes participated smoothly in the chloro-, bromo- and iodooxygenation (**6a**–**6f**). The vicinal brominated iminolactones (**6g**–**6i**) were obtained in 81–95% yields *via* 5- or 6-*exo* *O*-attacked cyclization. These results were consistent with the hard/soft acid–base theory (HSAB), where a carbocation as a hard acid was inclined to be attacked by a hard nucleophile with higher electronegativity.[23] The bromoxygenation of a 1,3-dicarbonyl compound, which contains an acidic proton and an olefinic side chain at an appropriate distance, allows the synthesis of highly functionalized cyclic ether **6j**. The successful construction of pyrrolidines (**8a**–**8c**) and *N*-sulfonate ester (**8d**) reveals the foundational synthetic competence of *N*-attacked cyclization. Notably, the bromocyclization of chiral alkene imidate **7e** afforded the exclusive diastereoselective formation of **8e** in 54% yield, the structure of which was determined by ^{1}H–^{1}H COSY.

Table 1 Optimization study[a]

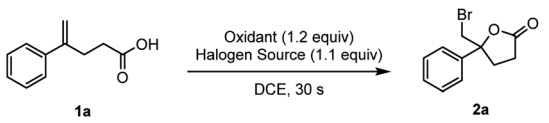

1a 2a

Entry	Oxidant	Halogen source	Yield[b] of **2a** [%]
1	PPO	TBAB	>96
2	MPO	TBAB	90
3	BPO	TBAB	<5[c] (90%)
4	LPO	TBAB	<5[c] (60%)
5	PPO	CsBr	13[c]
6	PPO	NBS	6[c]
7	PPO	TBAB	51[d]

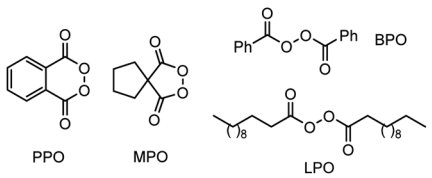

[a] Reaction conditions: **1a** (0.3 mmol, 1 equiv.), oxidant (0.36 mmol, 1.2 equiv.), Br source (0.33 mmol, 1.1 equiv.) in DCE (3 mL, 0.1 M) at room temperature, under an air atmosphere, 30 seconds. [b] Yields of isolated products after chromatographic purification. [c] Reaction time: 17 hours. [d] The reaction was performed with 400 nm LEDs (10 W). PPO = phthaloyl peroxide; BPO = benzoyl peroxide; MPO = malonoyl peroxide; LPO = lauroyl peroxide; TBAB = tetrabutylammonium bromide.

ICDA enhanced domino polyene-like halocyclization and gram-scale flow protocol

Due to the dual-anchoring orientation, the Br^{+} was transferred to the π-bond proximal to the carboxylic acid instead of the distal π-bond, resulting in the formation of mixed mono-cyclization products **10a** and **10a′** in 75% total yield. Conversely, without a strong hydrogen bond donor, the iodiranium-induced polyene cyclization furnished the corresponding bicyclic product **10b** in 67% yield when an electron-rich aryl served as

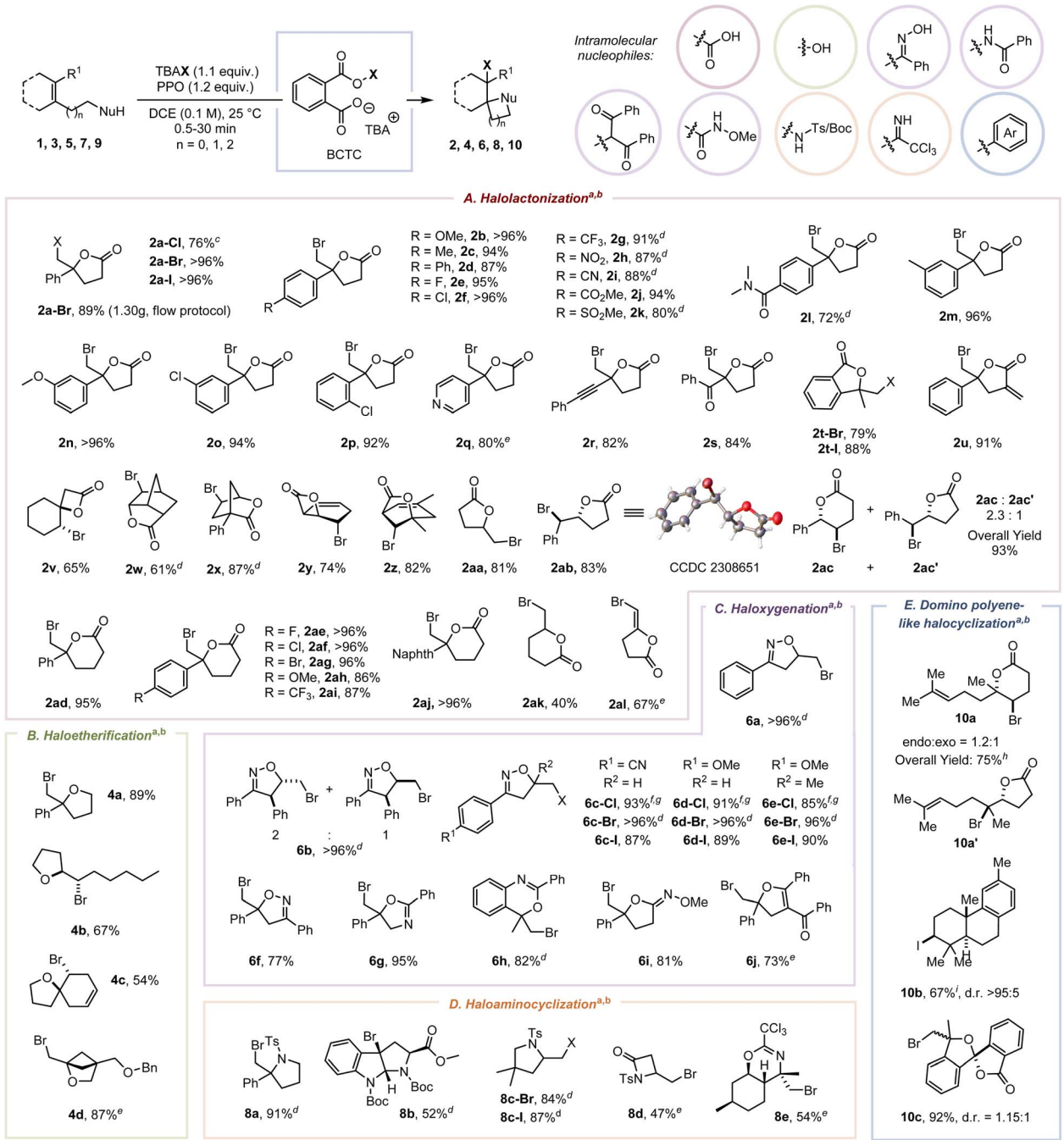

Scheme 2 Substrate scope for electrophilic halogenation of **1**, **3**, **5**, **7**, and **9** with BCTC. [a] Reaction conditions: olefin (0.3 mmol, 1 equiv.), PPO (0.36 mmol, 1.2 equiv.), TBAB (0.33 mmol, 1.1 equiv.) in DCE (3 mL, 0.1 M) at room temperature, under an air atmosphere, 30 seconds. [b] Yields of isolated products after chromatographic purification. [c] TBACl (2.2 equiv.) and PPO (2.2 equiv.) were used. [d] Reacted for 2 minutes instead of 30 seconds. [e] Reacted for 10 minutes instead of 30 seconds. [f] Reacted for 30 minutes instead of 30 seconds. [g] TBACl (3.0 equiv.) and PPO (3.0 equiv.) were used. [h] Reaction conditions: **9a** (0.1 mmol, 1 equiv.), HFIP (0.5 mmol, 5.0 equiv.), PPO (0.11 mmol, 1.1 equiv.), TBAB (0.11 mmol, 1.1 equiv.) in DCE (3.3 mL, 0.033 M) at −30 °C, under an air atmosphere, 5 minutes. [i] Reaction conditions: 9b (0.1 mmol, 1 equiv.), HFIP (1.5 mmol, 15.0 equiv.), PPO (0.11 mmol, 1.1 equiv.), TBAI (0.11 mmol, 1.1 equiv.) in DCE (5 mL, 0.02 M) at 0 °C, under an air atmosphere, 5 minutes. Ts = tosyl; Boc = *t*-butyloxy carbonyl; Tr = triphenyl; Bn = benzyl; Naphth = naphthyl; TBACl = tetrabutylammonium chloride, TBAI = tetrabutylammonium iodide, DCE = 1,2-dichloroethane.

the intramolecular nucleophile. Moreover, a spiroketal framework (**10c**, 1.15 : 1 d.r.) was constructed in 92% yield *via* halocyclization and spiroketalization.[4e] Recognizing the potential safety concerns associated with high-energy peroxide-containing compounds, we implemented the flow protocol to produce PPO through a packed bed reactor (Fig. S7 to S9†).[24] By combining with batch reaction, this approach allows a safer electrophilic bromolactonization to offer **2a-Br** (1.30 g, 89%

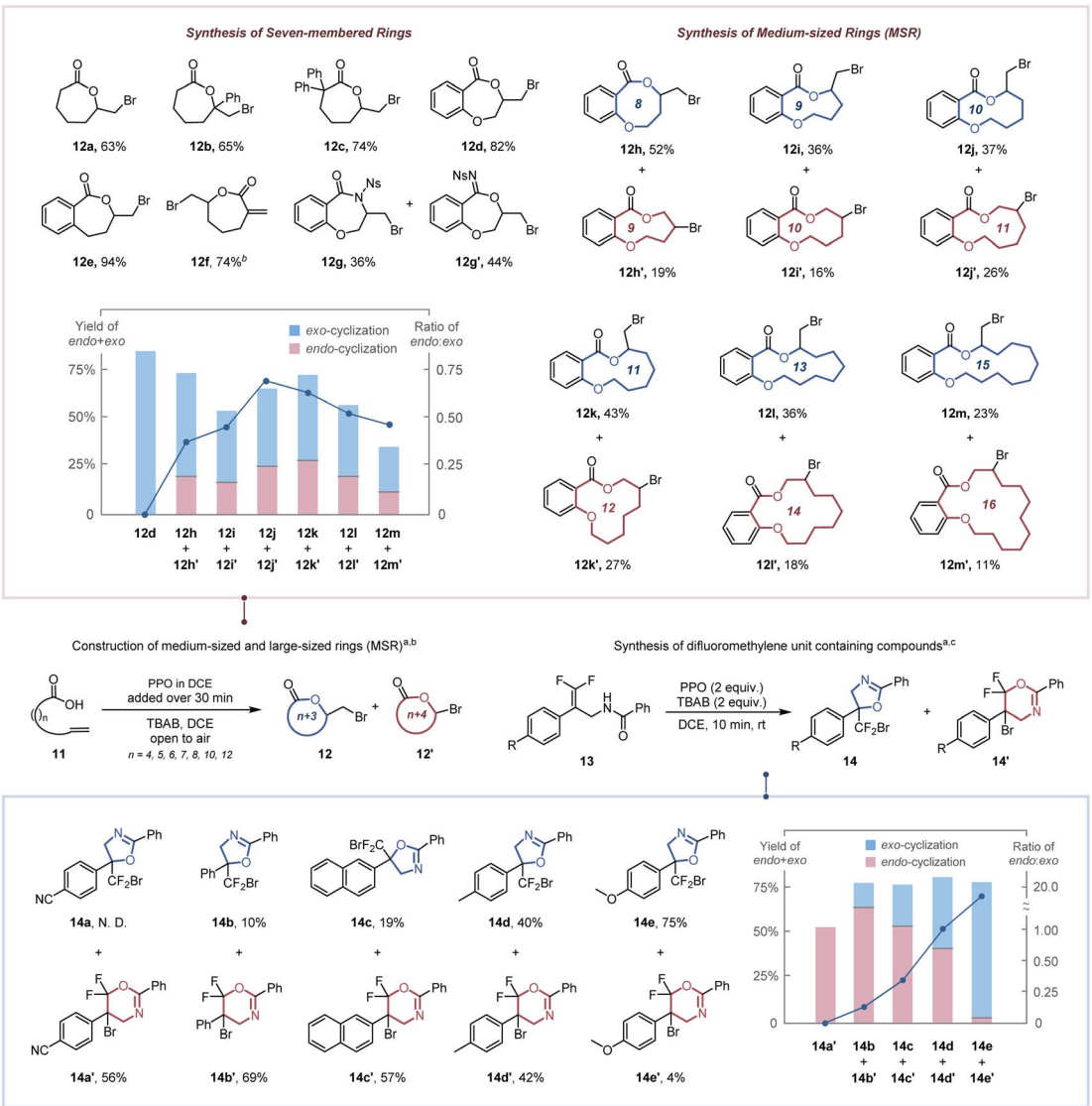

Scheme 3 Construction of medium-sized and large-sized rings and synthesis of difluoromethylene unit containing compounds. [a] Yields of isolated products after chromatographic purification. [b] Reaction conditions: olefin (0.3 mmol, 1 equiv.), PPO (0.60 mmol, 2.0 equiv.), TBAB (0.60 mmol, 2.0 equiv.) in DCE (15 mL, 0.02 M) at room temperature, under an air atmosphere, 30 minutes. [c] Reaction conditions: olefin (0.3 mmol, 1 equiv.), PPO (0.6 mmol, 2.0 equiv.), TBAB (0.6 mmol, 2.0 equiv.) in DCE (1 mL, 0.1 M) at room temperature, under an air atmosphere, 10 minutes. Ns = nosyl.

yield) by minimizing the accumulation of PPO and obviating the necessity for isolating and recrystallizing substantial quantities of PPO. Furthermore, a preliminary investigation into the enantioselective bromocyclization of **1a** and **7a** offered enantiomeric excesses (ee) of 25% and 36% with yields of 80% and 74%, respectively, when employing C11 as the chiral catalyst (Tables S6 and S7†).

Construction of medium-sized and large-sized rings and synthesis of a difluoromethylene unit containing compounds enhanced by ICDA

As a consequence of enthalpic (*e.g.*, transannular interactions, torsional and bond strains) and entropic influences,[25] the construction of seven-membered rings, medium-sized rings (MSR, typically eight-to-eleven membered rings) and large-sized rings is more challenging. Therefore, the high dilution and slow addition methodologies were utilized to reduce the competitive intermolecular addition (Table S5†).[26] The seven-membered *exo*-lactones (**12a–12f**) were obtained specifically in 63–92% yields (Scheme 3a). The inferior result obtained by replacing PPO with BPO demonstrates the importance of ICDA in the spatial adjustment of the reactive conformation for constructing medium-sized and large-sized rings (Table S5,† entry 6). Notably, our protocol has a clear advantage over previous reports in synthesizing seven-membered lactone **12d** (82% *vs.* 48%[2b] and 42%[2c]). The synthesis of seven-membered *α-exo*-methylene-lactone **12f**, which is critical for the anti-inflammatory exhibition of several natural and bioactive molecules,[27] was

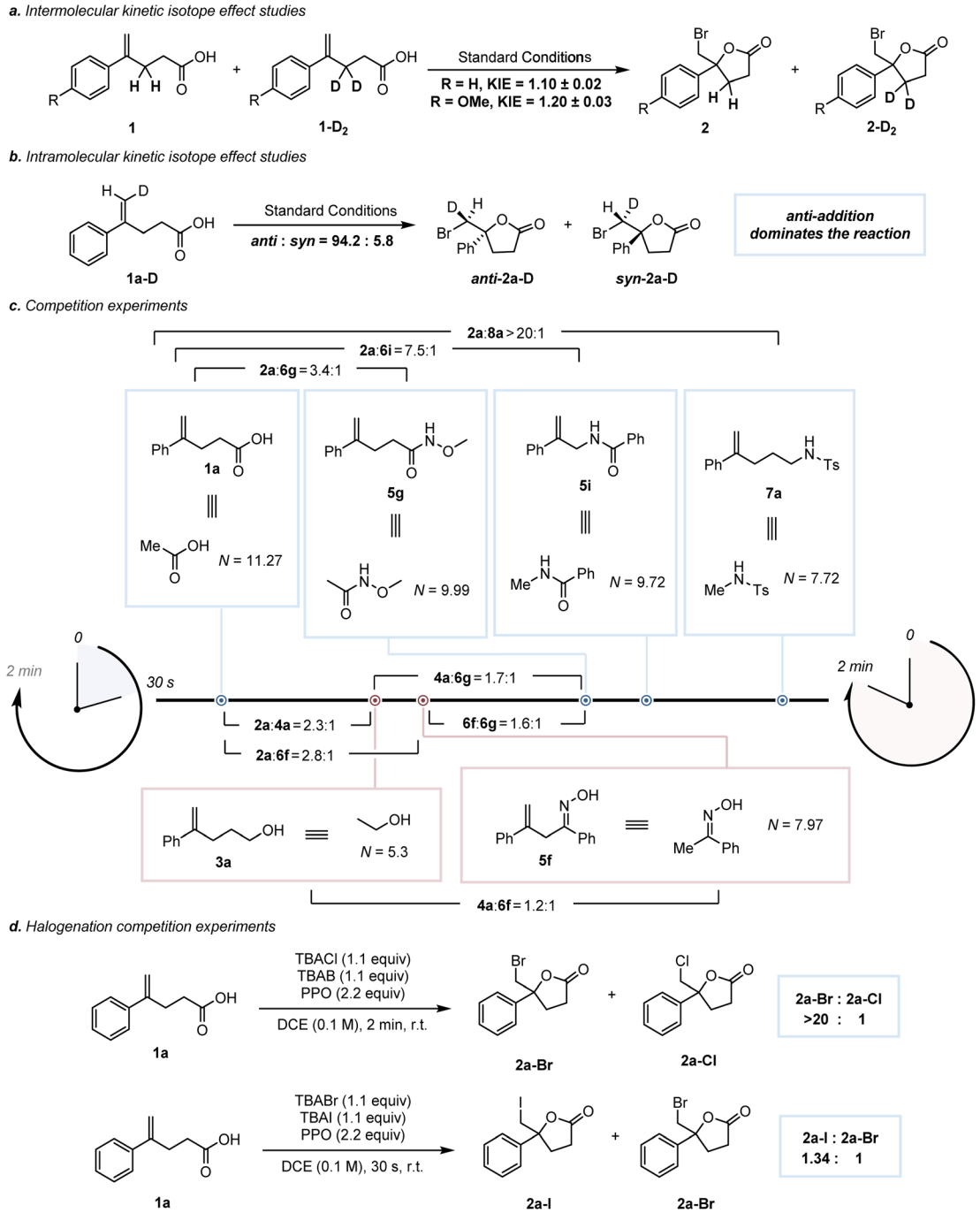

Scheme 4 KIE experiments and competition experiments.

accomplished in 74% yield. A competition of *O*-attacked and *N*-attacked cyclization was observed when **11g** was employed as a starting material, resulting in the generation of both *O*-cyclization product **12g** and *N*-cyclization product **12g′** in 36% and 44% yields, respectively. This may be due to that altering the substituent group from –OMe (electron-donating group) to –Ns (electron-withdrawing group) significantly increases the acidity of the relevant N–H bonds (the pK_a value in MeCN reduced from 19.08 to 16.05),[28] which accelerated the corresponding deprotonation process and the generation of the *N*-attacked cyclization product. For the construction of medium-sized and large-sized rings, both *endo*- and *exo*-cyclization products (**12h**–**12m′**) were observed in 34–71% total yields. The increase in the ratio of *endo* lactone with chain length ring sizes of 8–10 implies that the steric hindrance has a weaker effect in an *endo* approach than in an *exo* approach. Nevertheless, the transannular interaction[29] (H/H repulsions for methylene groups across the ring) was decreased for constructing larger rings while an increase of the *exo* lactone ratio was observed for chain lengths 11, 13 and 15. Our protocol was further applied to

access a tetrasubstituted difluoromethylene unit (Scheme 3b), which confers increased lipophilicity, oxidative stability and modulated bioavailability to pharmaceutical molecules.[30] Although it has been demonstrated that increasing the number of fluorine atoms on the π-bond could decrease its reactivity toward electrophilic reagents,[31] the desired difluoromethyl-containing oxazolines (**14a**–**14e**) could also be obtained *via exo*-cyclization or *endo*-cyclization in 56–82% total yields within 10 min.

Mechanism study

^{2}H KIE values were measured to investigate the reactive intermediate by considering two factors: (1) the adjacent C–H bonds of the carbenium ion center are expected to stabilize the carbon cation *via* the hyperconjugation effect; (2) the formation of the β-halo-carbenium ion should be slower in the labeled substrates **1a**-D_2 and **1b**-D_2 than in their parents (**1a** and **1b**).[32] The following ^{2}H KIE measurements for **1a**-D_2 and **1b**-D_2 were 1.10 and 1.20 (Scheme 4a), respectively. These values showed a β-secondary isotope effect and supported the presence of a β-halo-carbenium intermediate.[5a] To discriminate the face selectivity of nucleophilic attack during the reaction process, the bromolactonization of deuterated substrate **1a**-D was investigated (Scheme 4b).[33] As a consequence, the bromolactonization of **1a**-D under standard conditions led to **2a**-D with a significant predominance of an *anti* stereopreference (*anti* : *syn* = 94.2 : 5.8). The influence of the intramolecular nucleophile on the reaction rate of bromocyclization has been evaluated by intermolecular competition experiments.[34] **1a**, **3a**, **5f**, **5g**, **5i** and **7a** were subjected to competitive bromocyclization with others, respectively, and the resulting competition ratios are illustrated in Scheme 4c. According to the previous reports,[5a,35] we assumed that the differences in reaction rates were related to the nucleophilicity of the attacking group. For intramolecular reactions, knowledge of Baldwin's rules and effective molarity (EM) is required, that is, a correction term to adjust the prediction of the correlation equation to these processes.[36] Nevertheless, in light of the circumstance where the intramolecular reactions mentioned above undergo the same 5-*exo*-trig cyclization and involve the similar benzylic carbocation acceptors, we attempted to ignore the effect of the correction term[36] and utilized the nucleophilicity of the attacking groups to qualitatively evaluate the relative rate. The nucleophilicity parameters (*N*) of six molecules were predicted with the aid of the *r*SPOC model developed by Luo *et al.*,[37] and the reaction rates of **1a**, **5g**, **5i**, and **7a** show a positive correlation with the *N* values of their equivalents (Fig. S23,† top). The different ratios of **2a** *versus* **4a** in this work and a previous study,[5a] as well as the mismatches between the *N* values of **3a** and **5f** and the reaction rates (Scheme 4c, bottom), indicate that nucleophilicity is not the only factor influencing the reaction rate (Section S9.3). Next, the competition experiments of chlorolactonization, bromolactonization and iodolactonization showed that the iodolactonization was the fastest, while the chlorocyclization was the slowest (Scheme 4d, and Section S3), which may be due to the original difference in Lewis acidity of XB donors (I > Br > Cl).[38]

Density functional theory (DFT) calculations

Cation affinity evaluation has been widely applied under thermodynamically controlled conditions. For example, proton

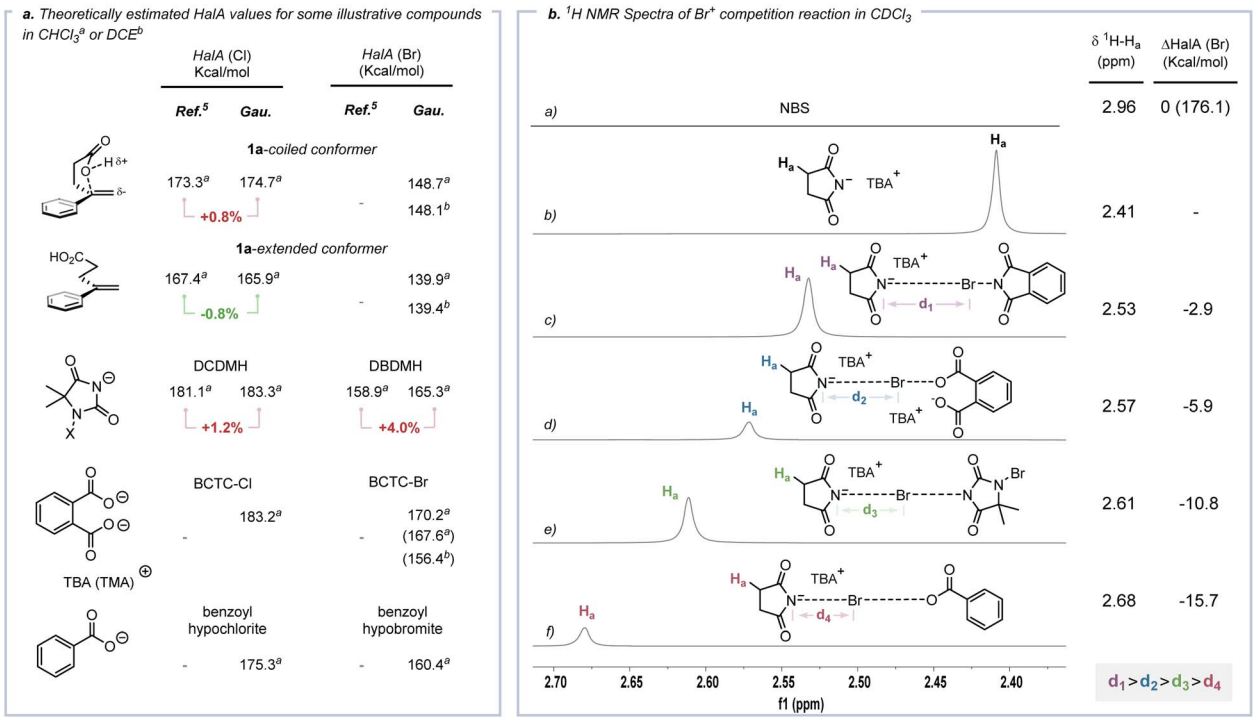

Scheme 5 *HalA* valuation.

affinity (PA) evaluation is important for rationalizing the biological functions of nucleic bases and designing hyperstrong neutral organic bases.[39] Analogously, Borhan *et al.* introduced halenium affinity (*HalA*) to quantificationally describe the bond strengths of various Lewis bases to X^+.[40] Recently, *HalA* evaluation has been employed to interpret, estimate and predict electrophilic halogenation reactions (Fig. S26†). Therefore, density functional theory (DFT) calculations (see the ESI† for details) were performed to evaluate the *HalA* scales of **1a**, anions of BCTC-X, benzoyl hypohalite (BPO-X) and commonly employed X^+ sources (Scheme 5a and Fig. S27a,† X = Cl and Br). The *HalA* value of the anion of BCTC-Br (170.2 kcal mol^{-1}) is higher than those of BPO-Br (160.4 kcal mol^{-1}) and DBDMH (165.3 kcal mol^{-1}) in $CHCl_3$. That is, the introduction of an intramolecular chaperone-like carboxylate anion slightly increases the O–Br bond strength of BCTC-Br. According to the definition of the *HalA* parameter, the anion with a higher *HalA* value has a greater ability to capture a Br^+, thus showing a stronger tendency to form the corresponding electrophilic bromination reagent. From this point of view, the intermolecular competition reactions of tetra-*n*-butylammonium succinimidate and electrophilic halogenation reagents were employed to visualize the Br^+ transfer. As shown in Scheme 5b, the chemical shift of $\mathbf{H_a}$ decreased from 2.41 ppm to 2.53, 2.57, 2.61 and 2.68 ppm when tetra-*n*-butylammonium succinimidate was mixed 1 : 1 with *N*-bromophthalimide (NBP), BCTC-Br, 1,3-dibromo-5,5-dimethylhydantoin (DBDMH) and BPO-Br, respectively. Namely, the capacity to capture Br^+ attenuated sequentially from NBP to BPO-Br, which accords with the *HalA*(Br) of the anion of NBS *versus* other anions (Δ*HalA*(Br) = −2.9, −5.9, −10.8 and −15.7 kcal mol^{-1}, Scheme 5b). The NPA charges of BPO-Br and BCTC-Br on the Br atom were calculated at the same level of theory and further proved the lower electrophilicity of the Br nucleus in BCTC-Br (Fig. S27c†). Comparing the *HalA*(Br) value of unactivated **1a** (139.4 kcal mol^{-1}) or nucleophile assisted alkene activation (NAAA)[5a] enabled **1a** (148.1 kcal mol^{-1}) with the anion of BCTC-Br (154.7 kcal mol^{-1}) in DCE, one would predict that simple Br^+ transfer to **1a** would be untenably endothermic (Δ*HalA*(Br) = −17.0 kcal mol^{-1}). In computational studies of the potential pathway, the ICDA affects the elongation of the O–Br bond and the conformation of the olefin, thus resulting in an effective Δ*HalA*(Br) (17.0 kcal mol^{-1}) relative to the unperturbed compounds (Scheme 6b). That is, the suitable preorganization overcame the

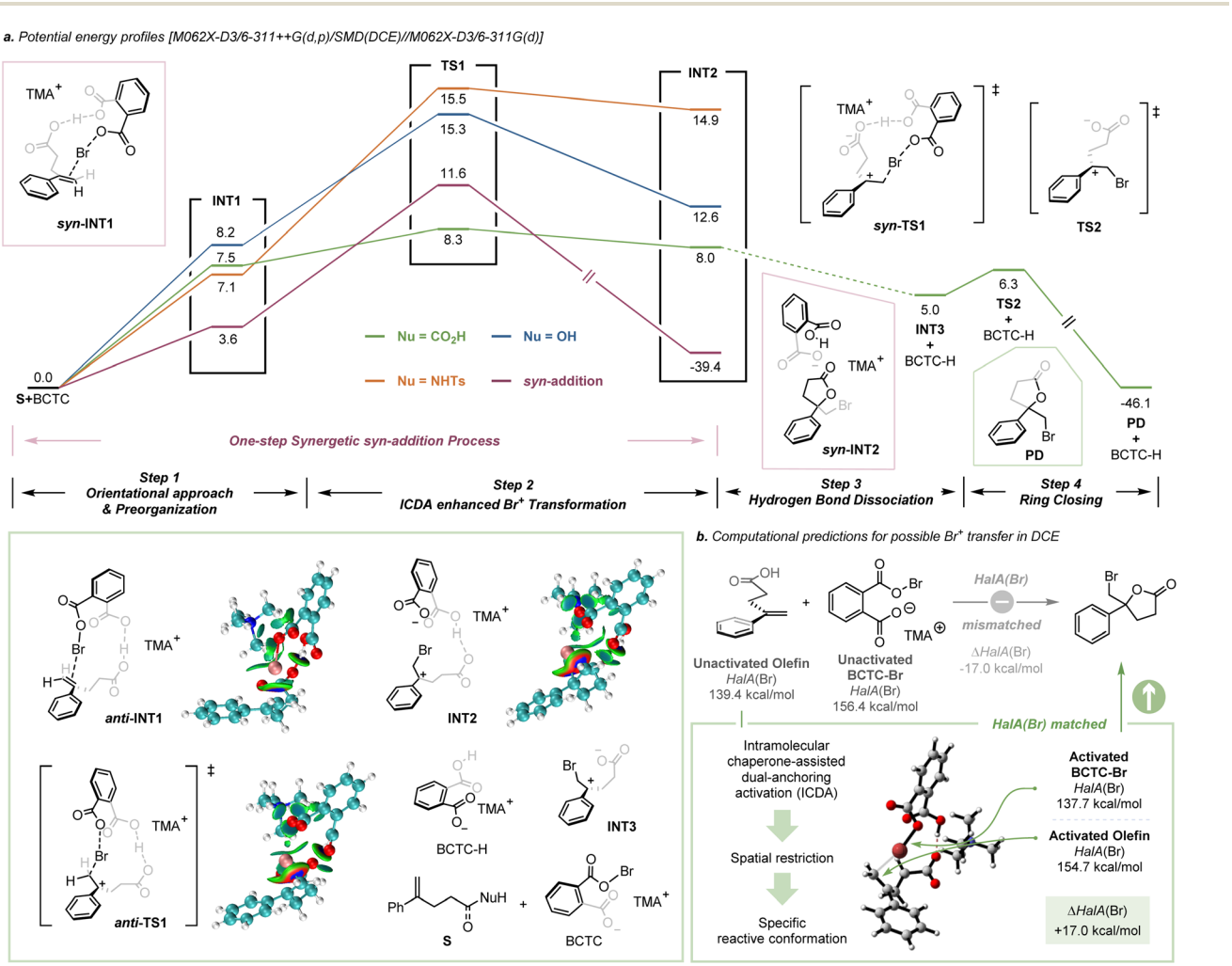

Scheme 6 Potential energy profiles and possible X^+ transfer *via HalA* prediction.

thermodynamic disadvantage of X^+ transfer. The reaction process depends not only on the nature of **1a** and BCTC, but also on the specific reactive conformation created in a precisely tailored environment.

DFT calculations were carried out to provide further insight into the mechanism of the ICDA enhanced electrophilic halocyclization (see the ESI† for details). As illustrated in Scheme 6a, the whole reaction consists of four steps. Orientational approach & preorganization: BCTC-Br approached the olefin *via* hydrogen bond interaction and the bromenium species was positioned in proximity to the π-bond. This preorganization process requires a certain amount of energy, which is less than 10 kcal mol^{-1}. ICDA enhanced Br^+ transfer: a cooperative activation of hydrogen bond and halogen bond interaction provided strict conformational control in a precisely tailored environment. Br^+ transfer takes place with a relatively small barrier (0.8 kcal mol^{-1}), which might be due to the preorganization process having pre-paid the entropy loss of the transition state. The rate-determining step is S+BCTC-Br → TS1. During the transfer of Br^+, it is obvious the halogen bond between the π-bond and Br^+ becomes stronger (Table S10†). In our calculations, three different substrates were chosen to study the effect of intramolecular nucleophiles. It is clear that for different nucleophilic groups, the reaction barrier changes, that is, for $-CO_2H$ it is the lowest, while for −NHTs it is the highest. Since the ^1H NMR experiments ruled out the possibility of hydrogen transfer as the initiation step (Fig. S28†), the hydrogen bond dissociation and ring closure take place successively after Br^+ transformation, with the O atom attacking the carbon cation from the opposite side. Furthermore, we found that the one-step *syn*-addition is thermodynamically unfavorable since its barrier is higher than that of the *anti*-addition process in our case, which is consistent with the intramolecular KIE experiment.

Conclusions

In conclusion, we have reported here a practical, versatile, catalyst-free and rapid electrophilic halocyclization that can afford structurally diversified valuable heterocyclic molecules in 30 s to 30 min. The synthetic ability can be categorized as follows: (a) synthesis of five-membered and six-membered substituted lactones, cyclic ethers, iminolactones and pyrrolidines, (b) domino polyene-like halocyclization, (c) a risk-reducing flow protocol for gram-scale synthesis, (d) construction of medium-sized and large-sized rings, (e) synthesis of difluoromethylene unit containing compounds, and (f) preliminary exploration of the catalytic asymmetric version. As shown in Fig. S30,† the ICDA enhanced halocyclization was demonstrated to be a powerful and superior protocol for the fast and high-yielding construction of seven types of heterocyclic units. DFT calculations verify the importance of suitable preorganization and the crucial role of the ICDA model in affording an induced-fit conformational change, stabilizing the transition state and accelerating X^+ transfer in the rate-determining step. The utilization of the ICDA model may open up straightforward access to fast, selective, and high-yielding synthetic transformations. Further development of new synthetic strategies is still underway in our laboratory.

Data availability

All data associated with this article are available from ESI.†

Author contributions

L. S. designed and directed the project. X. Y. performed the experiments and developed the reactions. X. Y. explored the substrate scope. X. Y. and H. G. developed the synthesis of substrates. H. G. and J. Y. helped in collecting some of the experimental data. X. Y. prepared the ESI.† J. Z. directed the DFT calculations. J. Z. and X. Y. performed DFT calculations and drafted the DFT sections. L. S. and X. Y. wrote the paper. All authors discussed the results and commented on the paper.

Conflicts of interest

There are no conflicts to declare.

Acknowledgements

This work was supported by the financial support from the National Natural Science Foundation of China (22271069, 21871067), the Guangdong Basic and Applied Basic Research Foundation (2023A1515012457, 2023A1515011332, 2021A1515010190), the State Key Laboratory of Urban Water Resources and Environment (Harbin Institute of Technology) (2022TS36), the Fundamental Research Funds for the Central Universities (HIT.OCET.2021035), Shenzhen Science and Technology Program (GXWD20231130100539001) and the Open Project Program of State Key Laboratory of Elemento-Organic Chemistry (202009). Computer time made available by the National Supercomputing Center of China in Shenzhen (Shenzhen Cloud Computing Center) is gratefully acknowledged. We deeply thank Prof. Herbert Mayr (Ludwig-Maximilians-Universität München) for providing suggestions for the intensive investigation of this research, Prof. Min Wang (Hangzhou Normal University) for the assistance with the measurement of High-Resolution Mass Spectrometry, and Dr Denghu Chang for the assistance and advice on the experimental operation.

Notes and references

1 (*a*) X.-W. Liang, C. Zheng and S.-L. You, *Chem.–Eur. J.*, 2016, **22**, 11918–11933; (*b*) S. A. Snyder, D. S. Treitler and A. P. Brucks, *Aldrichimica Acta*, 2011, **44**, 27–40; (*c*) S. E. Denmark and M. T. Burk, *Proc. Natl. Acad. Sci. U. S. A.*, 2010, **107**, 20655–20660; (*d*) C. Qi, G. Force, V. Gandon and D. Leboeuf, *Angew. Chem., Int. Ed.*, 2021, **60**, 946–953; (*e*) Q. Yin and S.-L. You, *Org. Lett.*, 2012, **14**, 3526–3529; (*f*) K. D. Ashtekar, H. Gholami, M. Moemeni, A. Chakraborty, L. Kiiskila, X. Ding, E. Toma, C. Rahn and B. Borhan, *Angew. Chem., Int. Ed.*, 2022, **61**, e202115173; (*g*)

M. Sofiadis, D. Xu, A. J. Rodriguez, B. Nissl, S. Clementson, N. N. Petersen and P. S. Baran, *J. Am. Chem. Soc.*, 2023, **145**, 21760–21765.

2 (*a*) Y. A. Cheng, W. Z. Yu and Y.-Y. Yeung, *J. Org. Chem.*, 2016, **81**, 545–552; (*b*) Y. A. Cheng, T. Chen, C. K. Tan, J. J. Heng and Y.-Y. Yeung, *J. Am. Chem. Soc.*, 2012, **134**, 16492–16495; (*c*) A. Verma, S. Jana, C. D. Prasad, A. Yadav and S. Kumar, *Chem. Commun.*, 2016, **52**, 4179–4182.

3 (*a*) A. M. Arnold, A. Pöthig, M. Drees and T. Gulder, *J. Am. Chem. Soc.*, 2018, **140**, 4344–4353; (*b*) S. A. Snyder, D. S. Treitler and A. P. Brucks, *J. Am. Chem. Soc.*, 2010, **132**, 14303–14314; (*c*) R. C. Samanta and H. Yamamoto, *J. Am. Chem. Soc.*, 2017, **139**, 1460–1463.

4 (*a*) S. E. Denmark, W. E. Kuester and M. T. Burk, *Angew. Chem., Int. Ed.*, 2012, **51**, 10938–10953; (*b*) J. Yan, Z. Zhou, Q. He, G. Chen, H. Wei and W. Xie, *Org. Chem. Front.*, 2022, **9**, 499–516; (*c*) Y. Lu, H. Nakatsuji, Y. Okumura, L. Yao and K. Ishihara, *J. Am. Chem. Soc.*, 2018, **140**, 6039–6043; (*d*) Y. M. Wang, J. Wu, C. Hoong, V. Rauniyar and F. D. Toste, *J. Am. Chem. Soc.*, 2012, **134**, 12928–12931; (*e*) T. Zheng, X. Wang, W.-H. Ng, Y.-L. S. Tse and Y.-Y. Yeung, *Nat. Catal.*, 2020, **3**, 993–1001; (*f*) K. Yamashita, R. Hirokawa, M. Ichikawa, T. Hisanaga, Y. Nagao, R. Takita, K. Watanabe, Y. Kawato and Y. Hamashima, *J. Am. Chem. Soc.*, 2022, **144**, 3913–3924; (*g*) D. C. Whitehead, R. Yousefi, A. Jaganathan and B. Borhan, *J. Am. Chem. Soc.*, 2010, **132**, 3298–3300; (*h*) M. T. Knowe, M. W. Danneman, S. Sun, M. Pink and J. N. Johnston, *J. Am. Chem. Soc.*, 2018, **140**, 1998–2001; (*i*) G. E. Veitch and E. N. Jacobsen, *Angew. Chem., Int. Ed.*, 2010, **49**, 7332–7335.

5 (*a*) K. D. Ashtekar, M. Vetticatt, R. Yousefi, J. E. Jackson and B. Borhan, *J. Am. Chem. Soc.*, 2016, **138**, 8114–8119; (*b*) R. Van Lommel, J. Bock, C. G. Daniliuc, U. Hennecke and F. De Proft, *Chem. Sci.*, 2021, **12**, 7746–7757.

6 I. Saikia, A. J. Borah and P. Phukan, *Chem. Rev.*, 2016, **116**, 6837–7024.

7 (*a*) W. Wang, X. Li, X. Yang, L. Ai, Z. Gong, N. Jiao and S. Song, *Nat. Commun.*, 2021, **12**, 3873; (*b*) S. D. Vaidya, S. T. Toenjes, N. Yamamoto, S. M. Maddox and J. L. Gustafson, *J. Am. Chem. Soc.*, 2020, **142**, 2198–2203; (*c*) M. C. Dobish and J. N. Johnston, *J. Am. Chem. Soc.*, 2012, **134**, 6068–6071; (*d*) X. He, X. Wang, Y.-L. S. Tse, Z. Ke and Y.-Y. Yeung, *Angew. Chem., Int. Ed.*, 2018, **57**, 12869–12873; (*e*) F. Mo, J. M. Yan, D. Qiu, F. Li, Y. Zhang and J. Wang, *Angew. Chem., Int. Ed.*, 2010, **49**, 2028–2032; (*f*) P. Zhou, L. Lin, L. Chen, X. Zhong, X. Liu and X. Feng, *J. Am. Chem. Soc.*, 2017, **139**, 13414–13419; (*g*) Y.-C. Chan and Y.-Y. Yeung, *Angew. Chem., Int. Ed.*, 2018, **57**, 3483–3487.

8 (*a*) A. Jaganathan, R. J. Staples and B. Borhan, *J. Am. Chem. Soc.*, 2013, **135**, 14806–14813; (*b*) X. Xiong and Y.-Y. Yeung, *Angew. Chem., Int. Ed.*, 2016, **55**, 16101–16105; (*c*) Z. Ke, C. K. Tan, F. Chen and Y.-Y. Yeung, *J. Am. Chem. Soc.*, 2014, **136**, 5627–5630; (*d*) Y. Nishii, M. Ikeda, Y. Hayashi, S. Kawauchi and M. Miura, *J. Am. Chem. Soc.*, 2020, **142**, 1621–1629; (*e*) Z. Tao, K. A. Robb, K. Zhao and S. E. Denmark, *J. Am. Chem. Soc.*, 2018, **140**, 3569–3573; (*f*) A. J. Cresswell, S. T.-C. Eey and S. E. Denmark, *Nat. Chem.*, 2015, **7**, 146–152; (*g*) A. Sakakura, A. Ukai and K. Ishihara, *Nature*, 2007, **445**, 900–903.

9 (*a*) S. A. Snyder, A. Gollner and M. I. Chiriac, *Nature*, 2011, **474**, 461–466; (*b*) S. A. Snyder, Z.-Y. Tang and R. Gupta, *J. Am. Chem. Soc.*, 2009, **131**, 5744–5745.

10 R. A. Rodriguez, C.-M. Pan, Y. Yabe, Y. Kawamata, M. D. Eastgate and P. S. Baran, *J. Am. Chem. Soc.*, 2014, **136**, 6908–6911.

11 J. Barluenga, M. Trincado, E. Rubio and J. M. González, *J. Am. Chem. Soc.*, 2004, **126**, 3416–3417.

12 S. A. Snyder and D. S. Treitler, *Angew. Chem., Int. Ed.*, 2009, **48**, 7899–7903.

13 J. C. Fontecilla-Camps and A. Volbeda, *Chem. Rev.*, 2022, **122**, 12110–12131.

14 K.-Y. Wang, J. Zhang, Y.-C. Hsu, H. Lin, Z. Han, J. Pang, Z. Yang, R.-R. Liang, W. Shi and H.-C. Zhou, *Chem. Rev.*, 2023, **123**, 5347–5420.

15 J. Latham, E. Brandenburger, S. A. Shepherd, B. R. K. Menon and J. Micklefield, *Chem. Rev.*, 2018, **118**, 232–269.

16 J. K. Nagle, *J. Am. Chem. Soc.*, 1990, **112**, 4741–4747.

17 C. Dong, S. Flecks, S. Unversucht, C. Haupt, K.-H. van Pée and J. H. Naismith, *Science*, 2005, **309**, 2216–2219.

18 (*a*) R. Zhao, K. Fu, Y. Fang, J. Zhou and L. Shi, *Angew. Chem., Int. Ed.*, 2020, **59**, 20682–20690; (*b*) R. Zhao, Y. Yao, D. Zhu, D. Chang, Y. Liu and L. Shi, *Org. Lett.*, 2018, **20**, 1228–1231.

19 N. London, D. Movshovitz-Attias and O. Schueler-Furman, *Structure*, 2010, **18**, 188–199.

20 X. Jiang, S. Liu, S. Yang, M. Jing, L. Xu, P. Yu, Y. Wang and Y.-Y. Yeung, *Org. Lett.*, 2018, **20**, 3259–3262.

21 T. Chen, T. J. Y. Foo and Y.-Y. Yeung, *ACS Catal.*, 2015, **5**, 4751–4755.

22 V. V. Levterov, Y. Panasyuk, V. O. Pivnytska and P. K. Mykhailiuk, *Angew. Chem., Int. Ed.*, 2020, **59**, 7161–7167.

23 H. Mayr, M. Breugst and A. R. Ofial, *Angew. Chem., Int. Ed.*, 2011, **50**, 6470–6505.

24 A. M. Eliasen, R. P. Thedford, K. R. Claussen, C. Yuan and D. A. Siegel, *Org. Lett.*, 2014, **16**, 3628–3631.

25 G. A. Molander, *Acc. Chem. Res.*, 1998, **31**, 603–609.

26 W. Zhao, Z. Li and J. Sun, *J. Am. Chem. Soc.*, 2013, **135**, 4680–4683.

27 T.-C. Tsai, H.-Y. Chen, J.-H. Sheu, M.-Y. Chiang, Z.-H. Wen, C.-F. Dai and J.-H. Su, *J. Agric. Food Chem.*, 2015, **63**, 7211–7218.

28 Q. Yang, Y. Li, J.-D. Yang, Y. Liu, L. Zhang, S. Luo and J.-P. Cheng, *Angew. Chem., Int. Ed.*, 2020, **59**, 19282–19291.

29 M.-C. Roux, R. Paugam and G. Rousseau, *J. Org. Chem.*, 2001, **66**, 4304–4310.

30 (*a*) E. Miller, S. Kim, K. Gibson, J. S. Derrick and F. D. Toste, *J. Am. Chem. Soc.*, 2020, **142**, 8946–8952; (*b*) W. K. Hagmann, *J. Med. Chem.*, 2008, **51**, 4359–4369; (*c*) N. A. Meanwell, *J. Med. Chem.*, 2018, **61**, 5822–5880; (*d*) A. P. Combs, *J. Med. Chem.*, 2010, **53**, 2333–2344; (*e*) Q. Zhou, A. Ruffoni, R. Gianatassio, Y. Fujiwara, E. Sella, D. Shabat and P. S. Baran, *Angew. Chem., Int. Ed.*, 2013, **52**, 3949–3952; (*f*) E. P. Gillis, K. J. Eastman, M. D. Hill, D. J. Donnelly and N. A. Meanwell, *J. Med. Chem.*, 2015, **58**, 8315–8359.

31 D. F. Shellhamer, J. L. Allen, R. D. Allen, D. C. Gleason, C. O'Neil Schlosser, B. J. Powers, J. W. Probst, M. C. Rhodes, A. J. Ryan, P. K. Titterington, G. G. Vaughan and V. L. Heasley, *J. Org. Chem.*, 2003, **68**, 3932–3937.
32 E. M. Simmons and J. F. Hartwig, *Angew. Chem., Int. Ed.*, 2012, **51**, 3066–3072.
33 R. Yousefi, K. D. Ashtekar, D. C. Whitehead, J. E. Jackson and B. Borhan, *J. Am. Chem. Soc.*, 2013, **135**, 14524–14527.
34 R. Huisgen, *Angew. Chem., Int. Ed.*, 1970, **9**, 751–762.
35 H. Mayr and A. R. Ofial, *Pure Appl. Chem.*, 2005, **77**, 1807–1827.
36 (*a*) L. Shi, M. Horn, S. Kobayashi and H. Mayr, *Chem.–Eur. J.*, 2009, **15**, 8533–8541; (*b*) J. E. Baldwin, *J. Chem. Soc. Chem. Commun.*, 1976, 734–736; (*c*) J. E. Baldwin, J. Cutting, W. Dupont, L. Kruse, L. Silberman and R. C. Thomas, *J. Chem. Soc. Chem. Commun.*, 1976, 736–738; (*d*) J. E. Baldwin, R. C. Thomas, L. I. Kruse and L. Silberman, *J. Org. Chem.*, 1977, **42**, 3846–3852; (*e*) C. D. Johnson, *Acc. Chem. Res.*, 1993, **26**, 476–482; (*f*) R. Cacciapaglia, S. Di Stefano and L. Mandolini, *Acc. Chem. Res.*, 2004, **37**, 113–122; (*g*) G. Illuminati and L. Mandolini, *Acc. Chem. Res.*, 1981, **14**, 95–102.
37 Y. Liu, Q. Yang, J. Cheng, L. Zhang, S. Luo and J.-P. Cheng, *ChemPhysChem*, 2023, **24**, e202300162.
38 R. L. Sutar and S. M. Huber, *ACS Catal.*, 2019, **9**, 9622–9639.
39 (*a*) Z. B. Maksić, B. Kovačević and R. Vianello, *Chem. Rev.*, 2012, **112**, 5240–5270; (*b*) K. Vazdar, D. Margetić, B. Kovačević, J. Sundermeyer, I. Leito and U. Jahn, *Acc. Chem. Res.*, 2021, **54**, 3108–3123.
40 K. D. Ashtekar, N. S. Marzijarani, A. Jaganathan, D. Holmes, J. E. Jackson and B. Borhan, *J. Am. Chem. Soc.*, 2014, **136**, 13355–13362.